REPORTS

PALEOMAGNETISM

Solar nebula magnetic fields recorded in the Semarkona meteorite

Roger R. Fu,[1]* Benjamin P. Weiss,[1] Eduardo A. Lima,[1] Richard J. Harrison,[2] Xue-Ning Bai,[3] Steven J. Desch,[4] Denton S. Ebel,[5] Clément Suavet,[1] Huapei Wang,[1] David Glenn,[6] David Le Sage,[7] Takeshi Kasama,[8] Ronald L. Walsworth,[6,7] Aaron T. Kuan[9]

Magnetic fields are proposed to have played a critical role in some of the most enigmatic processes of planetary formation by mediating the rapid accretion of disk material onto the central star and the formation of the first solids. However, there have been no experimental constraints on the intensity of these fields. Here we show that dusty olivine-bearing chondrules from the Semarkona meteorite were magnetized in a nebular field of 54 21 microteslas. This intensity supports chondrule formation by nebular shocks or planetesimal collisions rather than by electric currents, the x-wind, or other mechanisms near the Sun. This implies that background magnetic fields in the terrestrial planet-forming region were likely 5 to 54 microteslas, which is sufficient to account for measured rates of mass and angular momentum transport in protoplanetary disks.

Astronomical observations of young stellar objects indicate that early planetary systems evolve through a protoplanetary disk phase in <5 million years (My) following the collapse of their parent molecular clouds (1, 2). Disk evolution on such short time scales requires highly efficient inward transport of mass accompanied by outward angular momentum transfer, which allows disk material to accrete onto the central star while delivering angular momentum out of the protoplanetary system.

The mechanism of this rapid mass and angular momentum redistribution remains unknown. Several proposed processes invoke a central role for nebular magnetic fields. Among these, the magnetorotational instability (MRI) and magnetic braking predict magnetic fields with intensities of ~100 µT at 1 astronomical unit (AU) in the active layers of the disk (3, 4). Alternatively, transport by magnetocentrifugal wind (MCW) requires large-scale, ordered magnetic fields stronger than ~10 µT at 1 AU. Finally, nonmagnetic effects such as the baroclinic and Goldreich-Schubert-Fricke instabilities may be the dominant mechanism of angular momentum transport in the absence of sufficiently strong magnetic fields

(5). Direct measurement of magnetic fields in the planet-forming regions of the disk can potentially distinguish among and constrain these hypothesized mechanisms.
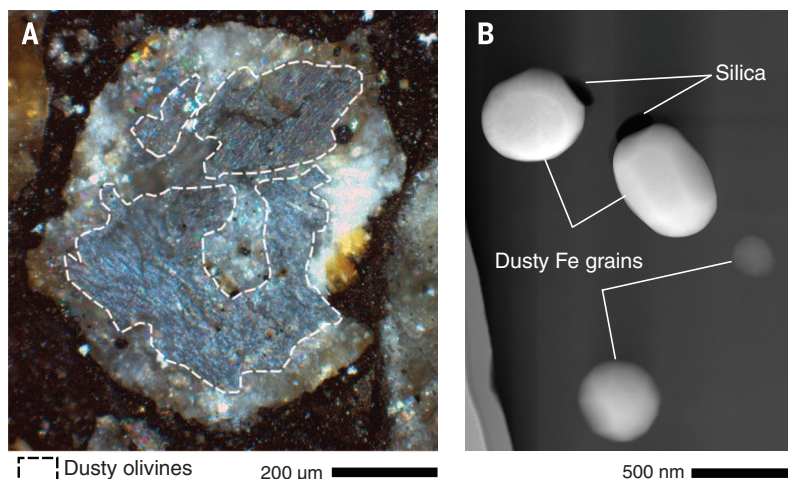
Although current astronomical observations cannot directly measure magnetic field strengths in planet-forming regions [(6, 7); supplementary text], paleomagnetic experiments on meteoritic materials can potentially constrain the strength of nebular magnetic fields. Chondrules

are millimeter-sized lithic constituents of primitive meteorites that formed in transient heating events in the solar nebula. If a stable field was present during cooling, they should have acquired a thermoremanent magnetization (TRM), which can be characterized via paleomagnetic experiments. Besides assessing the role of magnetic fields in disk evolution, such paleomagnetic measurements would constrain the currently unknown mechanism of chondrule formation.

Chondrules likely constituted a sizable fraction of the mass of asteroids and terrestrial planet precursors and may have facilitated the accretion of the first planetesimals (8, 9). The formation of chondrules therefore very likely represents a key stage in the evolution of the early solar system. The ambient magnetic field strength is a distinguishing characteristic among chondrule formation models. The x-wind model implies strong stellar fields of >80 to 400 µT (10). In contrast, magnetic fields in the nebular shock and planetesimal collision models are likely considerably lower than 100 µT (11, 12).

Previous paleomagnetic measurements of individual chondrules have focused mostly on the Allende CV chondrite (13). However, owing to extensive aqueous alteration on the CV parent body, magnetic phases in Allende chondrules are secondary and do not retain pre-accretional magnetization [i.e., magnetization acquired during the last heating of chondrules in the nebula and before the accretion of the meteorite's parent body; (14)]. Reliable recovery of preaccretional magnetization requires samples that have avoided appreciable postaccretional remagnetization processes.

Among the most pristine known meteorites is the Semarkona LL3.00 ordinary chondrite. We conducted paleomagnetic studies on Semarkona,

[1]Department of Earth, Atmospheric and Planetary Sciences, Massachusetts Institute of Technology (MIT), Cambridge, MA, USA. [2]Department of Earth Sciences, University of Cambridge, Cambridge, UK. [3]Hubble Fellow, Harvard-Smithsonian Center for Astrophysics, Cambridge, MA, USA. [4]School of Earth and Space Exploration, Arizona State University, Tempe, AZ, USA. [5]Department of Earth and Planetary Sciences, American Museum of Natural History (AMNH), New York, NY, USA. [6]Harvard-Smithsonian Center for Astrophysics, Cambridge, MA, USA. [7]Department of Physics, Harvard University, Cambridge, MA, USA. [8]Center for Electron Nanoscopy, Technical University of Denmark, Kongens Lyngby, Denmark. [9]School of Engineering and Applied Science, Harvard University, Cambridge, MA, USA.
*Corresponding author. E-mail: rogerf@mit.edu

Fig. 1. Dusty olivine-bearing chondrules from the Semarkona meteorite. (A) Optical photomicrograph of chondrule DOC4 showing the location of dusty olivine grains. Image taken in reflected light with crossed polarizers. (B) Annular dark-field scanning transmission electron microscope (STEM) image of four dusty olivine Fe grains from chondrule DOC5. Brightness in image reflects column-averaged atomic number; darker grains are smaller in size, implying a higher relative abundance of olivine at their location and hence a lower mean atomic number. The euhedral morphology and chemical homogeneity of the Fe grains is apparent, which indicate the lack of secondary recrystallization and alteration. Such Fe grains are the primary carriers of preaccretional magnetization in Semarkona chondrules.

focusing in particular on dusty olivine-bearing chondrules (Fig. 1). Dusty olivine crystals consist of submicrometer–sized grains of nearly pure body-centered cubic (bcc) Fe (kamacite) embedded in forsteritic olivine (15). Such olivine grains are found in approximately 1 in 10 chondrules in ordinary chondrites.

Because of their unique compositional and magnetic properties, dusty olivine grains are expected to retain preaccretional magnetization. The small grain size of dusty olivine metal implies that most are in the single domain (SD) or single vortex (SV) states, which can retain stable magnetization over the history of the solar system (16–19). Further, the Ni-poor composition (Ni <2 weight %) of dusty olivine metal precludes metamorphic recrystallization (15, 20). The domain states of dusty olivine metals imply very high coercivities ranging up to >200 mT, as confirmed by our demagnetization experiments (see below). The magnetization of grains with such high coercivities should not have been much altered by the low shock pressures likely experienced by Semarkona [4 to 10 GPa (21, 22)]. Finally, the low porosities of the surrounding olivine crystals have protected metal from aqueous alteration (Fig. 1B).

The distinctive, high coercivities of dusty olivine grains allow for the isolation of their remanent magnetization during alternating field (AF) demagnetization as larger (10 to 100 μm) mesostasis metal grains are expected to demagnetize at AF levels <50 mT (23). Furthermore, because the postaccretional peak metamorphic temperature of Semarkona was likely only 200° to 260°C (24, 25), preaccretional remanence in dusty olivine metals should be isolated upon laboratory (1 hour duration) thermal demagnetization to <450°C assuming that metamorphism lasted ~5 My (16, 19). In summary, no known postaccretional process is likely to have compromised preaccretional remanent magnetization in Semarkona dusty olivines; strong-field AF demagnetization or thermal demagnetization above ~450°C is expected to isolate the preaccretional component of magnetization.

We isolated eight dusty olivine-bearing chondrules from two 15 mm by 10 mm by 150 μm–thick sections of Semarkona provided by the American Museum of Natural History (AMNH). Both sections contain fusion crust along one edge. We also extracted 5 non-dusty olivine-bearing chondrules and 29 bulk (i.e., mixed matrix and chondrule) samples to characterize any postaccretional overprints. All extracted samples are mutually oriented to within 5°. Owing to their weak moments [natural remanent magnetization (NRM) ranging between 10^{-10} and 3×10^{-12} A·m² before demagnetization], chondrules were measured with the superconducting quantum interference device (SQUID) microscope (26, 27) at the MIT Paleomagnetism Laboratory (Fig. 2). Supporting magnetic imaging measurements with higher spatial resolution were performed with a nitrogen-vacancy (NV) quantum diamond microscope (supplementary text).

Bulk samples were subjected to AF demagnetization up to 85 to 145 mT or thermal demagnetization up to 580°C. We identified three unidirectional postaccretional overprints in our Semarkona samples: two low coercivity (LCa and LCb) and one medium coercivity (MCa) components. Twenty bulk samples carry the LCa overprint blocked up to between 4.5 and 13 mT (Fig. 3). This component is present in both fusion crust material and meteorite interior samples, indicating that it was acquired after arrival on Earth. Removal of the LCa magnetization during thermal demagnetization to only 70°C indicates that it is likely a viscous remanent magnetization (VRM) acquired during long-term exposure to the Earth's field.

In contrast, the MCa overprint is only present in samples within 4.7 mm of the fusion crust. The mean paleointensity of this component based on the isothermal remanent magnetization (IRM) and anhysteretic remanent magnetization (ARM) normalization methods (76 μT) is within uncertainty of the Earth's magnetic field. We conclude
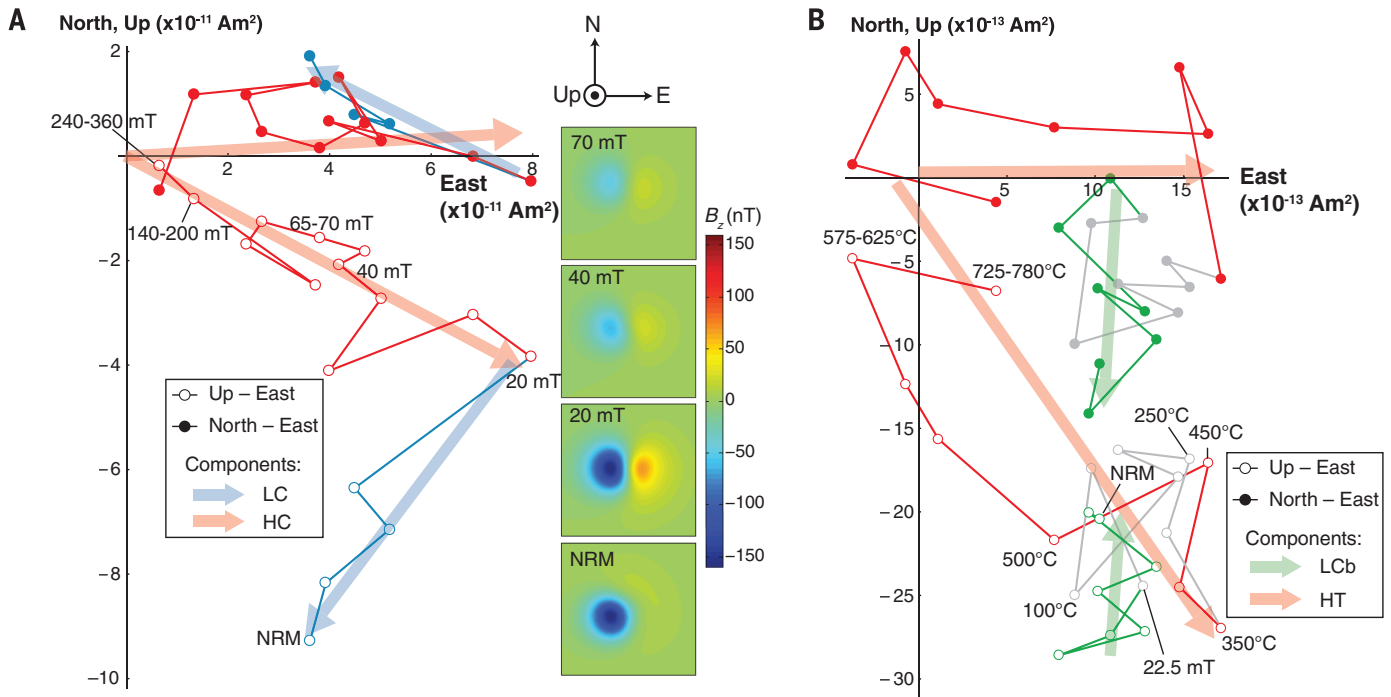
Fig. 2. AF and thermal demagnetization of single dusty olivine-bearing chondrules measured with SQUID microscopy. Orthogonal projection diagrams showing the evolution of the natural remanent magnetization (NRM) of two chondrules upon progressive demagnetization. Open and solid circles indicate the projection of the NRM vector onto the vertical (up-east) and horizontal (north-east) planes, respectively. (**A**) AF demagnetization of DOC1 reveals a low coercivity (LC) overprint removed by 20 mT and higher coercivity (HC) magnetization that persists to >290 mT while decaying in magnitude toward the origin. Insets show associated magnetic field maps measured with the SQUID microscope at the indicated demagnetization levels where positive (red) field values are in the up direction. The stable directionality and steady decay of the magnetization can be seen during AF application above 20 mT. (**B**) Mixed AF and thermal demagnetization of DOC8 shows the removal of the postaccretional LCb overprint by 20.0 mT (green points), a stationary moment between room temperature and ~400°C (gray), and an origin-trending high temperature (HT) component removed by 780°C (red). Steps above 40 mT or 575°C have been averaged to suppress noise.

that the MCa component was acquired during heating from atmospheric passage. Finally, a small subset of seven samples from one edge of our Semarkona section carry the LCb overprint, which is completely removed by AF demagnetization up to between 10.5 and 30 mT. The high intensity of the LCb component (NRM to saturation IRM ratio of 0.23) suggests that it was acquired during exposure to artificial magnetic fields. Only two dusty olivine-bearing chondrules carried the LCb overprint, which was fully removed upon AF application to 20 mT. To summarize, all samples >1.0 mm from the fusion crust, which include all dusty olivine-bearing chondrules, do not carry any postaccretional remagnetization other than the LCa, MCa, and LCb components. These overprints, if present, are readily identified and removed via AF cleaning.

Eight dusty olivine-bearing chondrules were subjected to AF and thermal demagnetization up to 290 to 420 mT or 780°C. Six of these were found to carry a high coercivity (HC) or high temperature (HT) component of magnetization. We argue based on seven lines of evidence that these HC/HT components are preaccretional TRMs (supplementary text). (i) HC/HT components decay to the origin upon demagnetization, which is the expected behavior of primary magnetization (Fig. 2). (ii) The HC/HT magnetization directions in the six chondrules are collectively random, passing the conglomerate test at the 95% confidence level [Fig. 3; (28)]. No HC/HT component is oriented in the direction of any of the postaccretional overprints. (iii) The HC magnetizations in chondrules DOC3 and DOC4, which were each partitioned into two subsamples, are unidirectional within each chondrule and inconsistent with random magnetizations at the 99% confidence level. Such uniformity is expected of a TRM acquired by individual chondrules cooling in the solar nebula because the field should be uniform across the submillimeter scale of each sample (14). (iv) The blocking temperature range of the HT component (350° to 750°C) agrees closely with that expected of a preaccretional magnetization that was partially demagnetized for ~5 My at ~200°C [Fig. 2B; (16, 19)], which is the estimated metamorphic temperature for Semarkona on the LL parent body (16, 25). (v) Magnetic field maps of dusty olivine-bearing chondrules confirm that the HC magnetization is carried by dusty olivines, which formed in the nebula and are expected to retain preaccretional magnetization as outlined above. (vi) The magnetization direction acquired during cooling for a spinning chondrule is expected to be parallel to its rotation axis (29). The close alignment between the HC directions and the short axes of our chondrules, which are likely related to the rotation axis (supplementary text), are nonrandom at the 98% confidence level, suggesting that HC/HT magnetizations were indeed acquired parallel to the spin axis. (vii) The coercivity spectrum of the HC component of dusty olivine-bearing chondrules is very similar to that of an ARM and dissimilar to that of an IRM, which suggests that the HC component was acquired as a TRM (30). We therefore conclude with high confidence that the HC/HT magnetizations observed in dusty olivine-bearing chondrules are TRMs acquired in the solar nebula.

TRM acquisition experiments on analogs of dusty olivine chondrules have shown that the ARM normalization method potentially produces paleointensities accurate to ~40% [2σ; (30)]. Assuming that the five chondrules with recovered paleointensities formed in similar magnetic field conditions in the nebula, our nominal ARM paleointensities for six dusty olivines yielded a mean value of 27 μT. The morphology of chondrules (31) and the apparent correspondence between HC magnetization directions and the short axes of our chondrule samples (see above paragraph) strongly suggest that chondrules were rotating during remanence acquisition in the solar nebula. In the case of rotation around a single axis, which is the expected motion inherited from cooling of a viscous droplet, the true mean field intensity should have been greater than our experimental paleointensity by a factor of 2 (supplementary text). Meanwhile, precession of the chondrule's rotation axis would imply a multiplicative factor of up to 4. However, given the high inferred rotation rates of chondrules (>50 s^{-1}), the magnitudes of effects that may lead to precession are comparatively small. Therefore, we adopt nonprecessing rotation as the most likely state of cooling chondrules and recommend a value of 54 ± 21 μT (2σ) for the ambient nebular field strength. Although unlikely, if chondrules did not rotate or precessed strongly during remanence acquisition, the corresponding estimated ambient field strength would be 27 ± 8 μT or 108 ± 42 μT (2σ), respectively.

Our paleointensity constrains the magnetic field environment during the last time the chondrule cooled through the 765° to 350°C blocking temperature range of the HC/HT component, which likely was the chondrule-forming event. Our recommended paleointensity is significantly lower than the >80 to 400 μT expected for chondrules purportedly formed in the x-wind model (10). Furthermore, mechanisms that invoke intense electric currents such as magnetic reconnection flares and current sheets predict strong fields >500 μT during chondrule heating (32). The short-circuit instability may also imply similarly strong fields at high temperature (33), although the decay of field strength below 765°C has not been studied in detail. In contrast, assuming that magnetic fields inherited from the collapsing molecular cloud were on the order of 10 μT (12), nebular shocks, which may enhance the ambient magnetic field by a factor of <10, would result in paleointensities of <100 μT (11). Meanwhile, planetesimal collisions would likely not perturb the background field. Therefore, nebular shocks and planetesimal collisions are the chondrule formation models most consistent with our measured paleointensities.

Adopting nebular shocks and planetesimal collisions as the most likely origins of chondrules, background magnetic fields in the nebula may have been amplified by a factor between 1 and 10 during chondrule formation. We therefore infer that background magnetic fields in the solar nebula were between 5 and 54 μT (11). Assuming Semarkona chondrules formed near 2.5 AU, which is the present-day location of S-type asteroids (34), the vertical distribution of dust in the nebula strongly suggests that

Fig. 3. Magnetization directions in Semarkona chondrules and bulk samples. Equal area stereonet projection diagram where colored points denote high coercivity or high temperature (HC/HT) magnetization in individual dusty olivine-bearing sample or subsamples. Circles indicate the associated maximum angular deviation (MAD) obtained from principle components analysis. Each color represents a single chondrule with chondrules DOC3 and DOC4 having two subsamples each. Black stars and associated ovals represent the mean directions of the three postaccretional overprints identified from bulk samples and their 95% confidence intervals. Open symbols represent the upper hemisphere; solid symbols represent the lower hemisphere. The wide scatter of the HC/HT magnetizations, the unidirectionality of subsamples from DOC3 and DOC4, and their noncorrespondence to the directions of postaccretional overprints provide strong evidence for a preaccretional origin of the HC/HT magnetizations in dusty olivine-bearing chondrules.
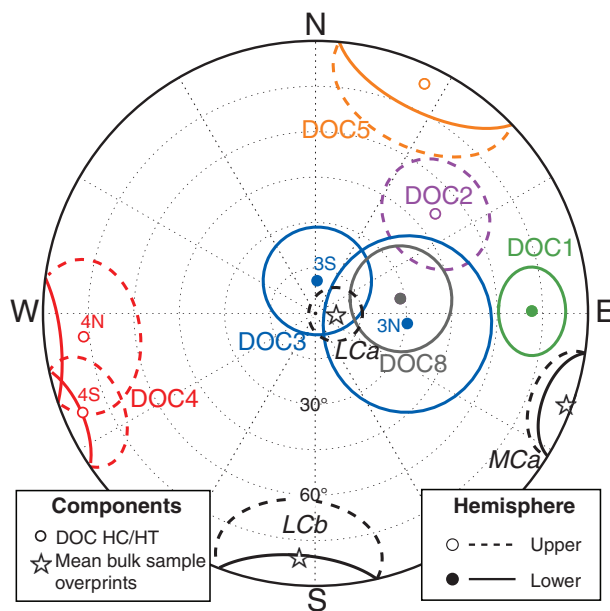
chondrule formation took place in the weakly ionized "dead zone," which contains gas poorly coupled to local magnetic fields and occurs within ~3 gas scale heights of the midplane (35). Our measurements therefore indicate that a substantial magnetic field [yet still well below the ~400 μT equipartition field strength (3)] existed in the dead zone, potentially as a result of fields inherited from the collapse of the solar system's parent molecular cloud. Given our measured field strengths, mass accretion driven by the MRI or magnetic braking at 2.5 AU would have been $<0.04 \times 10^{-8}$ to 3.5×10^{-8} M_{sun} year^{-1}, where M_{sun} is the Sun's mass (supplementary text). Meanwhile, the MCW model would predict mass accretion rates of 0.3×10^{-7} to 30×10^{-7} M_{sun} year^{-1} or less. The inferred age of Semarkona chondrules is 2 to 3 My after the first calcium aluminum–rich inclusions (36). Given that protoplanetary disks are observed to have accretion rates of 10^{-9}-10^{-7} M_{sun} year^{-1} at 2 to 3 My after collapse of their parent molecular clouds (2), both magnetic mechanism could fully account for the expected accretion rates. This suggests that magnetic fields govern the observed rapid transformation of protoplanetary disks into planetary systems around Sun-like stars.

REFERENCES AND NOTES

1. K. E. Haisch Jr., E. A. Lada, C. J. Lada, Astrophys. J. 553, L153–L156 (2001).
2. L. Hartmann, N. Calvet, E. Gullbring, P. D'Alessio, Astrophys. J. 495, 385–400 (1998).
3. M. Wardle, Astrophys. Space Sci. 311, 35–45 (2007).
4. X.-N. Bai, J. Goodman, Astrophys. J. 701, 737–755 (2009).
5. N. J. Turner, S. Fromang, C. Gammie, H. Klahr, G. Lesur, M. Wardle, X.-N. Bai, in Protostars and Planets VI (Univ. of Arizona Press, Tucson, AZ, 2014).
6. R. M. Crutcher, Annu. Rev. Astron. Astrophys. 50, 29–63 (2012).
7. I. W. Stephens et al., Nature 514, 597–599 (2014).
8. J. N. Cuzzi, R. C. Hogan, K. Shariff, Astrophys. J. 687, 1432–1447 (2008).
9. T. Nakamura et al., Science 333, 1113–1116 (2011).
10. F. H. Shu, H. Shang, T. Lee, Science 271, 1545–1552 (1996).
11. S. J. Desch, H. C. Connolly Jr., Meteorit. Planet. Sci. 37, 183–207 (2002).
12. S. J. Desch, T. C. Mouschovias, Astrophys. J. 550, 314–333 (2001).
13. N. Sugiura, D. W. Strangway, Proc. Lunar Planet. Sci. Conf. 15th, C729 (1985).
14. R. R. Fu, E. A. Lima, B. P. Weiss, Earth Planet. Sci. Lett. 404, 54–66 (2014).
15. H. Leroux, G. Libourel, L. Lemelle, F. Guyot, Meteorit. Planet. Sci. 38, 81–94 (2003).
16. M. Uehara, N. Nakamura, Earth Planet. Sci. Lett. 250, 292–305 (2006).
17. S.-C. L. L. Lappe et al., Geochem. Geophys. Geosyst. 12, Q12Z35 (2011).
18. M. Winklhofer, K. Fabian, F. Heider, J. Geophys. Res. 102, 22695 (1997).
19. I. Garrick-Bethell, B. P. Weiss, Earth Planet. Sci. Lett. 294, 1–7 (2010).
20. R. J. Reisener, J. I. Goldstein, in Lunar Planet. Sci. Conf. XXX (Lunar and Planetary Institute, Houston, TX, 1999), pp. 1868.
21. D. Stöffler, K. Keil, E. R. D. Scott, Geochim. Cosmochim. Acta 55, 3845 (1991).
22. R. R. Fu et al., Science 338, 238–241 (2012).
23. J. Gattacceca et al., Meteorit. Planet. Sci. 49, 652–676 (2014).
24. C. M. O. D. Alexander, D. J. Barber, R. Hutchison, Geochim. Cosmochim. Acta 53, 3045–3057 (1989).
25. G. D. Cody et al., Earth Planet. Sci. Lett. 272, 446–455 (2008).
26. B. P. Weiss, E. A. Lima, L. E. Fong, F. J. Baudenbacher, J. Geophys. Res. 112, B09105 (2007).
27. E. A. Lima, B. P. Weiss, R. R. Fu, A. C. Bruno, in AGU Fall Meeting (San Francisco, 2013), vol. GP43B-07.
28. G. S. Watson, Mon. Not. R. Astron. Soc. 7, 160–161 (1956).
29. C. Suavet, J. Gattacceca, P. Rochette, L. Folco, Geology 39, 123–126 (2011).
30. S.-C. L. L. Lappe, J. M. Feinberg, A. Muxworthy, R. J. Harrison, Geochem. Geophys. Geosyst. 14, 2143–2158 (2013).
31. H. Miura, T. Nakamoto, M. Doi, Icarus 197, 269–281 (2008).
32. E. H. Levy, S. Araki, Icarus 81, 74–91 (1989).
33. C. P. McNally, A. Hubbard, M.-M. Mac Low, D. S. Ebel, P. D'Alessio, Astrophys. J. 767, L2 (2013).
34. S. J. Bus, R. P. Binzel, Icarus 158, 146–177 (2002).
35. X.-N. Bai, Astrophys. J. 739, 50 (2011).
36. S. Mostefaoui et al., Meteorit. Planet. Sci. 37, 421–438 (2002).

MATERIALS SCIENCE

Dynamic mechanical behavior of multilayer graphene via supersonic projectile penetration

Jae-Hwang Lee,[1,2]* Phillip E. Loya,[1] Jun Lou,[1] Edwin L. Thomas[1]*

Multilayer graphene is an exceptional anisotropic material due to its layered structure composed of two-dimensional carbon lattices. Although the intrinsic mechanical properties of graphene have been investigated at quasi-static conditions, its behavior under extreme dynamic conditions has not yet been studied. We report the high–strain-rate behavior of multilayer graphene over a range of thicknesses from 10 to 100 nanometers by using miniaturized ballistic tests. Tensile stretching of the membrane into a cone shape is followed by initiation of radial cracks that approximately follow crystallographic directions and extend outward well beyond the impact area. The specific penetration energy for multilayer graphene is ~10 times more than literature values for macroscopic steel sheets at 600 meters per second.

G raphene, the atomic monolayer building block of graphite, is known for its exceptionally high intrinsic strength and stiffness arising from the two-dimensional (2D) hexagonal lattice of covalently bonded carbon atoms. Recently, graphene's in-plane Young's modulus ($Y_\parallel$) was measured to be more than 1.0 TPa using atomic force microscope nanoindentation (1). Because tensile mechanical stresses in a material cannot be transmitted faster than the speed of sound [$c \sim (Y/\rho)^{1/2}$, where ρ is the density of the material], the nonequilibrium local stress arising from the inertial effect becomes important under dynamic conditions accompanying high–strain-rate, predominantly tensile loading (2). In this regard, the relatively low density (~2200 kg m^{-3}) of graphene (3), along with its high modulus, leads to a superior in-plane speed of sound ($c_\parallel \sim 22.2$ km s^{-1}), implying that concentrated stresses applied under extreme conditions can rapidly be delocalized.

Nanoindentation has served as an effective technique to study the tensile mechanical properties of monolayer graphene. It is inherently a low-speed test (<<1 m s^{-1}), but strain rates can reach ~10^5 to 10^6 s^{-1} for very thin samples (4), whereas most high-speed, high–strain-rate mechanical characterization techniques, such as split-Hopkinson pressure bar (5) and ballistic tests (6), are inappropriate for testing very thin specimens. To address high-speed and high–strain-rate tensile-dominated penetration of thin films, we improved our laser-induced projectile impact test (LIPIT) (7). In this advanced LIPIT (or "α-LIPIT"), a single micrometer-size solid silica sphere (or "μ-bullet") is fired at a high speed

[1]Department of Materials Science and NanoEngineering, Rice University, Houston, TX 77005, USA. [2]Department of Mechanical and Industrial Engineering, University of Massachusetts, Amherst, MA 01003, USA.
*Corresponding author. E-mail: leejh@umass.edu (J.-H.L.); elt@rice.edu (E.L.T.)